



Tendamistat surface accessibility to the TEMPOL paramagnetic probe

Maria Scarselli^a, Andrea Bernini^a, Claudia Segoni^a, Henriette Molinari^b, Gennaro Esposito^c, Arthur M. Lesk^d, Franco Laschi^e, Pierandrea Temussi^f & Neri Niccolai^{a,*}

^aDipartimento di Biologia Molecolare and Centro per lo Studio Strutturale di Sistemi Biomolecolari, Università di Siena, Via A. Fiorentina 1, I-53100 Siena, Italy; ^bIstituto Policattedra, Università di Verona, I-37100 Verona, Italy; ^cDipartimento di Scienze e Tecnologie Biomediche, Università di Udine, I-33100 Udine, Italy; ^dDepartment of Haematology, University of Cambridge, Cambridge CB2 2QH, U.K.; ^eDipartimento di Chimica, Università di Siena, I-53100 Siena, Italy; ^fDipartimento di Chimica, Università di Napoli, I-80134 Napoli, Italy

Received 22 April 1999; Accepted 3 August 1999

Key words: molecular presentation, protein structure, spin-labels, surface accessibility, tendamistat

Abstract

TEMPOL, the soluble spin-label 4-hydroxy-2,2,6,6-tetramethyl-piperidine-1-oxyl, has been used to determine the surface characteristics of tendamistat, a small protein with a well-characterised structure both in solution and in the crystal. A good correlation has been found between predicted regions of exposed protein surface and the intensity attenuations induced by the probe on 2D NMR TOCSY cross peaks of tendamistat in the paramagnetic water solution. All the high paramagnetic effects have been interpreted in terms of more efficient competition of TEMPOL with water molecules at some surface positions. The active site of tendamistat coincides with the largest surface patch accessible to the probe. A strong hydration of protein N and C termini can also be suggested by this structural approach, as these locations exhibit reduced paramagnetic perturbations. Provided that the solution structure is known, the use of this paramagnetic probe seems to be well suited to delineate the dynamic behaviour of the protein surface and, more generally, to gain relevant information about the molecular presentation processes.

Introduction

Intermolecular recognition, suitably driven by a favourable topological presentation, is the primary event for the biological activity of any molecule. Elucidating the mechanisms of recognition and binding processes, a chain of events still hardly predictable, is crucial for rational protein engineering.

NMR has proven to be a powerful tool for investigating molecular structure and dynamics of protein systems (Wüthrich, 1998). A unique feature of protein NMR is the possibility of performing detailed studies of hydration by observing intermolecular nuclear Overhauser effects (Otting et al., 1990, 1991; Clore et al., 1990). The technique can be very efficient for monitoring protein surface accessibility, without the problems that may arise in the crystal from molecu-

lar trapping at protein–protein interfaces. Hydration of the protein surface is not uniform, a feature that may reflect a differential accessibility to molecules other than water, e.g., the presence of preferential binding sites for substrates, inhibitors or even exogenous aspecific ligands. The possibility of monitoring the presence of putative binding sites for small cosolvent molecules on the protein surface helps to delineate general trends in the molecular recognition process and is complementary to information on surface solvation. In this respect, recent studies, carried out both in solution (Liepinsh et al., 1997; Dalvit et al., 1998; Dalvit, 1999) and in the crystal state (Ringe, 1995; Mattos et al., 1996), have pointed out that proteins have one or more molecular regions where small and uncharged organic molecules, very different also from physiological ligands, preferentially approach the molecular surface. This finding is very general and can be ascribed to a reduced strength in the competi-

*To whom correspondence should be addressed. E-mail: niccolai@unisi.it

tive binding of water molecules to these regions. Thus, it is possible to propose that accurate mapping of the accessibility of the protein surface may help to locate the main interaction points. If one takes into account the fact that regions exhibiting such propensities always include the protein active site, it is possible to envisage a sort of vortex effect that contributes to the efficiency and precision of ligand binding.

Such an effect may be rationalised in terms of cooperativity within the pathway of consecutive events involving ligand sampling approach, reorientation, solvent displacement, non-covalent interactions etc., that eventually lead to binding, the component driving forces being of van der Waals, electrostatic, hydrophobic and hydrophilic type.

NMR spectroscopy may monitor these surface processes through Overhauser or isotope exchange measurements. However, the high concentration of diamagnetic chemical probes required by Overhauser effect experiments could partially modify the protein surface composition, while the amide protons which are located at the protein surface most often exchange too fast for an accurate quantitative analysis. Thus, additional NMR methods are required. The technique of adding to the solvent the stable free radical TEMPOL (4-hydroxy-2,2,6,6-tetramethyl-piperidine-1-oxyl), previously proposed for topological mappings of protein surfaces (Esposito et al., 1989, 1993; Petros et al., 1990; Niccolai et al., 1991; Molinari et al., 1997), seems very promising for defining the dynamics of the protein surface accessibility. The donor/acceptor capability of hydrogen bonds of TEMPOL makes this spin-probe more similar to water molecules, i.e. less biased towards hydrophobic moieties of the protein surface, with respect to other nitroxides, such as TEMPO or TEMPONE. Also due to the absence of any electric charge on this molecule, preferential interactions with particular residues could be excluded in a model unfolded peptide (Esposito et al., 1993). As a final remark, it should be noted that a sizeable reduction of selected signal intensities may be reached at TEMPOL concentrations that do not perturb the conformational stability of the investigated proteins.

Here we present the application of the TEMPOL approach to tendamistat, a protein whose surface has been well characterised both in solution (Kline et al., 1985; Billeter et al., 1989) and in the crystal (Pflugrath et al., 1986). An additional interesting feature of tendamistat is the fact that, being itself the inhibitor of a larger protein, it has a single active site (Marchius

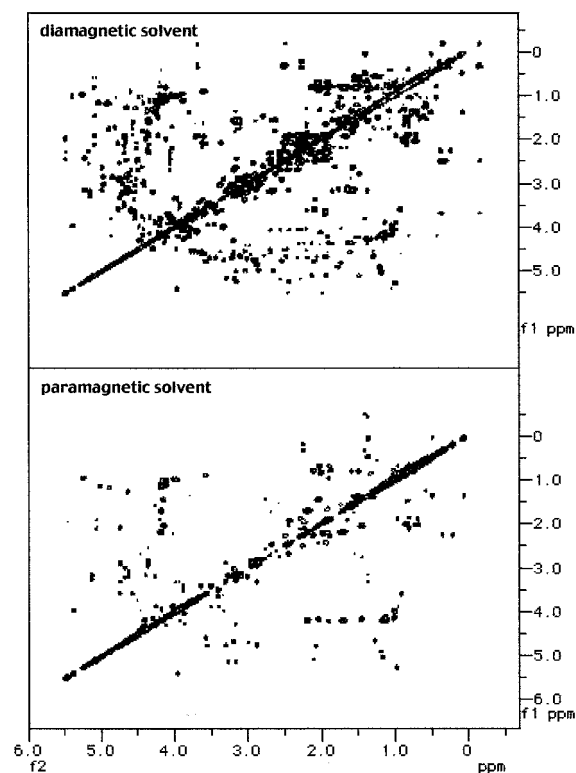


Figure 1. The ^1H NMR TOCSY spectra of the aliphatic region of 5 mM tendamistat obtained at 600 MHz, in D_2O and at 50°C in the presence and in the absence of 50 mM TEMPOL.

et al., 1996). This circumstance rules out interferences from secondary binding sites that might occasionally be found on the surface of a large protein capable of interacting with several small ligands.

Experimental procedures

Tendamistat was kindly offered by Hoechst AG and purified by reverse phase HPLC. TEMPOL, obtained from Sigma, was used without any further manipulation. ESR measurements of 1 mM water solutions of TEMPOL at 25°C and 50°C , in the absence and in the presence of tendamistat at concentrations of 2 and 0.1 mM have been performed on a Bruker 200 D SRC X band spectrometer. The NMR samples contained 5 mM tendamistat in D_2O and an optimal TEMPOL concentration was achieved at 50 mM. This condition was reached by adding directly to the NMR tube a few microliters of a 2 M TEMPOL solution. Proton NMR spectra, run at 50°C to reproduce the experimental conditions of the original structural study (Kline

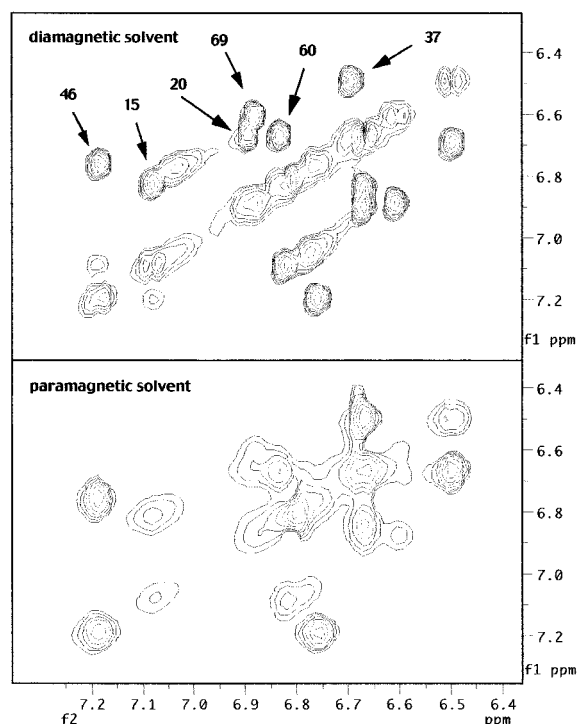


Figure 2. The tyrosyl aromatic region of the ^1H NMR TOCSY spectra of tendamistat obtained in the presence and in the absence of TEMPOL and under the same experimental conditions as described in Figure 1.

et al., 1986), were acquired at 600 MHz on a Bruker AMX spectrometer. Standard pulse sequences were used to obtain TOCSY spectra (Rance, 1987) with mixing times of 54 ms. The water resonance was attenuated using a DANTE presaturation train (Morris et al., 1978) superimposed to the specific sequences. A total of 470 increments were collected in t_1 with 1908 data points and 64 scans/FID in t_2 , over a spectral width of 6 KHz in both dimensions. Prior to 2D FT the experimental array was zero-filled to a final matrix of 2048×1024 data points. Chemical shifts were referred to the most upfield-shifted methyl resonance of the molecule, set at 0.12 ppm (Kline et al., 1986). NMR data were processed with an X32 workstation, using UXNMR software and with a Macintosh G3 with the SwaN-MR software (Balacco, 1994). As previously reported (Molinari et al., 1997), paramagnetic effects were measured by comparing autoscaled cross-peak attenuation figures, A_i , defined as:

$$A_i = [2 - (v_{ip}/v_{id})] \quad (1)$$

i.e. the individual deviations from the average of the cross-peak autoscaled volumes, $v_{ip,d}$, the latter defined as:

$$v_{ip,d} = V_{ip,d} / [(1/n)(\sum_i V_{ip,d})] \quad (2)$$

where n is the number of measured cross-peak volumes and V_{id} and V_{ip} are the protein individual cross-peak volumes measured in the absence and in the presence of the spin-probe, respectively. The individual A_i 's were plotted versus protein sequence position and the values lying above or below the average attenuation level, unitary by construction because $(\sum_i v_{ip,d}/n) = 1$, correspond respectively to high or low spin-probe accessibility levels (Molinari et al., 1997). With this representation it is easy to compare experiments performed under different conditions (temperature, protein and paramagnetic probe concentration, solvents), since any general effect is included in the mean value and the observed deviations. Due to the experimental errors in measuring the cross-peak volumes, the standard deviation analysis defines the range of confidence of the attenuation data. Therefore, only the paramagnetic attenuation values outside the standard deviation are worth considering. For non-equivalent methylene protons a mean attenuation value was reported. A_i values have been compared to the sum of the autoscaled exposed surface areas (ESA_i) (Molinari et al., 1997). The exposed surface area, esa_i , calculated with a program implemented by A.M. Lesk, in analogy to the A_i definition was used to obtain the corresponding autoscaled value:

$$ESA_i = \left(\frac{esa_i - \sum_{i=1}^n esa_i/n}{\sum_{i=1}^n esa_i/n} \right) \quad (3)$$

For each methyl and methylene group the sum of the individual hydrogen exposures was considered.

Results and discussion

It has been already established (Esposito et al., 1989, 1993; Petros et al., 1990; Niccolai et al., 1991; Molinari et al., 1997) that resonance attenuations induced by TEMPOL on 2D cross peaks may yield significant information on protein structure, provided that (i) no preferential interaction between the spin-probe and the macromolecule occurs, and (ii) the analysis is carried out on nuclei which experience similar chemical environments and dynamics. When these conditions are met, the electron-nucleus dipolar interactions, responsible for the paramagnetic perturbations, readily

reflect the different average exposure to the spin-probe of the various molecular regions. In the present study we intend to somehow refine these statements, which, while still generally valid, may prove too simplistic when the overall paramagnetic perturbation of the protein spectra is considered. Especially for the paramagnetic attenuation of the side-chain resonances, resorting to mobility differences to relieve the task of a quantitative analysis hinders altogether a piece of experimental information that may be quite relevant to address the very problem of protein surface accessibility. Although disregarding paramagnetic effects on side-chain resonances appears largely justified by the complexity of accurate proton relaxation studies, an attempt to recover the information encoded by these data is worth trying. We have thus decided to consider the paramagnetic perturbation of the protein NMR spectra without restricting the discussion only to the backbone resonances. This approach is conducted in terms of local trends within different classes of hydrogen resonances.

To investigate the surface accessibility of tendamistat to TEMPOL, a preliminary ESR study of water solutions containing the paramagnetic probe and the protein has been carried out. The different concentrations employed in this exploratory study reproduce the experimental conditions of the NMR studies, but extend the concentration range in order to evidence possible TEMPOL complexation at low spin-probe/protein ratios. All the ESR spectra, obtained in the presence and in the absence of tendamistat, are typical of a freely tumbling nitroxide (Campbell et al., 1984) with the three sharp lines of nearly equal intensities. The ESR parameters measured under the various experimental conditions, reported in Table 1, suggest that, at most, only very weak interactions occur between the paramagnetic probe and the protein. The interaction of the paramagnetic probe TEMPOL with tendamistat can therefore be analysed in terms of transient association of the spin-probe with the accessible surface sites of the protein.

This study has been carried out under the same experimental conditions as the previous structural determination study of tendamistat (Kline et al., 1986) and, as expected, the measured proton chemical shifts were consistent with the reported data.

A 50 mM TEMPOL concentration ensures a sizeable broadening of tendamistat proton signals without losing too much S/N ratio and all the attenuation data reported here refer to this experimental condition. Since denaturing effects of TEMPOL on the

protein could not be excluded a priori, particularly at the used high temperature and concentration, after each addition of the 1 M solution of TEMPOL to the 5 mM tendamistat solution, 1D tendamistat spectra were recorded to check for spectral modifications. Thus, at the final 50 mM concentration of the paramagnetic probe, all residues exhibit chemical shift changes of the α protons lower than 0.03 ppm with the exception of D1, D58 and L74, with upfield shifts of 0.06 ppm, while C27, D39 and H64 show downfield shifts of 0.04 ppm. These small chemical shift changes confirm that conformational perturbations, if present, affect only a small fraction of the protein molecules.

The aliphatic and aromatic regions of the TOCSY map of tendamistat, recorded in diamagnetic and paramagnetic water solutions, are shown in Figures 1 and 2, respectively. A decreased number of scalar connectivities in the presence of TEMPOL is readily seen, as well as the appearance of intense cross peaks from the spin-probe protons at 4.17, 2.06 and 1.47 ppm.

It should be noted here that this spin-probe concentration, required for optimal *paramagnetic shock* to the tendamistat proton relaxation, is higher than in previous studies at room temperature, in agreement with the dynamics of the investigated molecular system. It has been proposed (Niccolai et al., 1982), indeed, that the molecular diffusion modulates the dipolar interactions between the protein protons and the paramagnetic probe and, therefore, the higher the temperature, the less effective is the paramagnetic contribution to the proton relaxation process.

As mentioned in the Experimental section, for a meaningful assessment of paramagnetic effects, A_i values can be profitably compared to exposed surface areas. Exposed surface areas, ESA_i , have been calculated with probe radii of 1.4 and 4.4 Å, corresponding to water and TEMPOL molecules respectively, using the tendamistat hydrogen coordinates of the NMR-derived structure of the Protein Data Bank (PDB code 4AIT; Kline et al., 1988). However, the comparison with A_i data is shown only for accessibilities calculated for the water molecule, since the mesh obtained using a 4.4 Å in the surface sampling is too coarse. In this respect it should be emphasised that TEMPOL cannot be considered as a purely mechanical NMR probe. The spin-probe effects on the proton resonance intensities are, in fact, due to through-space interactions and, hence, do not necessarily entail direct atomic contacts, as this paramagnetic perturbation can propagate up to 15 Å from the position of the unpaired electron (Girvin et al., 1995).

Table 1. ESR parameters measured for TEMPOL (10^{-3} M) at 25 °C and 50 °C

| | 25 °C | | | 50 °C | | |
|------|------------------|------------------|------------|------------------|------------------|------------|
| | g_{iso} | a_{iso} | ΔH | g_{iso} | a_{iso} | ΔH |
| f | 2.0050(4) | 34.04(4) | 1.7(4) | 2.0054(4) | 17.4(4) | 1.9(0) |
| 10/1 | 2.0050(7) | 34.04(3) | 1.7(4) | 2.0055(2) | 17.4(4) | 1.9(0) |
| 1/2 | 2.0055(4) | 34.04(4) | 1.7(4) | 2.0060(4) | 17.0(4) | 1.8(5) |

Values given were obtained for the free spin-probe (f), in the presence of 10^{-4} M tendamistat (10/1) and 2×10^{-3} M tendamistat (1/2). ΔH and a_{iso} are both expressed in Gauss. Values in parentheses are outside the estimated range of confidence of the data.

The temperature factors reported in the NMR restrained PDB file of tendamistat (4AIT) describe the root-mean-square deviations (rmsd) of the individual atoms of the structures II to IX relative to structure I of the atom records (Kline et al., 1988). Structure I, in turn, is the coordinate set with the minimum global deviation from the NMR restraints. It is possible, therefore, to discuss the correlation between A_i and ESA_i also by taking into account the undetermined shape of the protein surface due to local flexibility (backbone and/or side chain). The coordinates of structure I were used for model building and ESA_i calculations while the rmsd values of the individual hydrogen atom positions of the related hydrogens were considered for evaluating the confidence range of the exposure factors for the surface atoms of the molecule, see Figures 3 and 4. It should be noted that the NMR solution structure of tendamistat exhibits good conformational definition. Structure I, with the exception of the four N-terminal residues, fits quite closely the remaining ones, as long as the backbone is considered. When all the heavy atoms are taken into account, however, the rmsd values indicate side chain flexibility for several residues, particularly for the ones located in the active site.

When considering the intensity variations of TOCSY cross peaks in response to the paramagnetic perturbation, a different contribution from each of the two protons which cause a given J connectivity in the cross-peak intensity should be expected, in principle. However, in agreement with previous suggestions (Molinari et al., 1997), the sum of the ESA_i 's of the nuclei which cause a J connectivity is considered in the present report to discuss the correlation of the computed surface exposure with the paramagnetic attenuations.

TOCSY spectra of tendamistat show a large variety of well-resolved cross peaks and it is easy to identify

many homologous J connectivities from the different types of residues. To reduce possible ambiguities in the analysis of the NMR data, only the paramagnetic attenuations of non-overlapping 2D cross peaks were considered. In the case of non-equivalent methylene protons, mean attenuations have been reported. Thus, the attenuations of 90 J connectivities can be measured and analysed with two different grouping criteria. In the first grouping, the same types of connectivity for a given amino acid are compared, see Figure 3, in order to exclude possible contributions to the TEMPOL-induced effects which could arise from specific characteristics of each residue type. On the other hand, by the second criterion, a comparison is made among the paramagnetic attenuations of all the detected α - β J connectivities, as shown in Figure 4, to probe the paramagnetic attenuations of protons with an expectedly similar reorientation rate which should reflect the overall protein motion. The local dynamics of the TEMPOL-tendamistat interaction, indeed, might be critical for the resulting A_i .

As a general remark on the 90 paramagnetic effects of Figures 3 and 4, it can be observed that the calculated attenuations strongly differ for the various connectivities. In order to define confidence range limits for data analysis, the standard deviation, σ , of all A_i values was calculated. Assuming that the limits of an average paramagnetic perturbation extend over $\pm\sigma/2$ around the theoretical value of the average attenuation, the obtained value of $\sigma = 0.54$ identifies three A_i regions, namely (i) high paramagnetic effects with $A_i > 1.27$, (ii) average behaviours with $1.27 \geq A_i \geq 0.73$ and (iii) weak paramagnetic effects with $A_i < 0.73$. The analysis of the paramagnetic effects falling outside the defined average behaviour range limits the discussion to only 63 attenuation values.

The least perturbed correlations by the paramagnetic probes are: (i) the α and β hydrogen connectivity

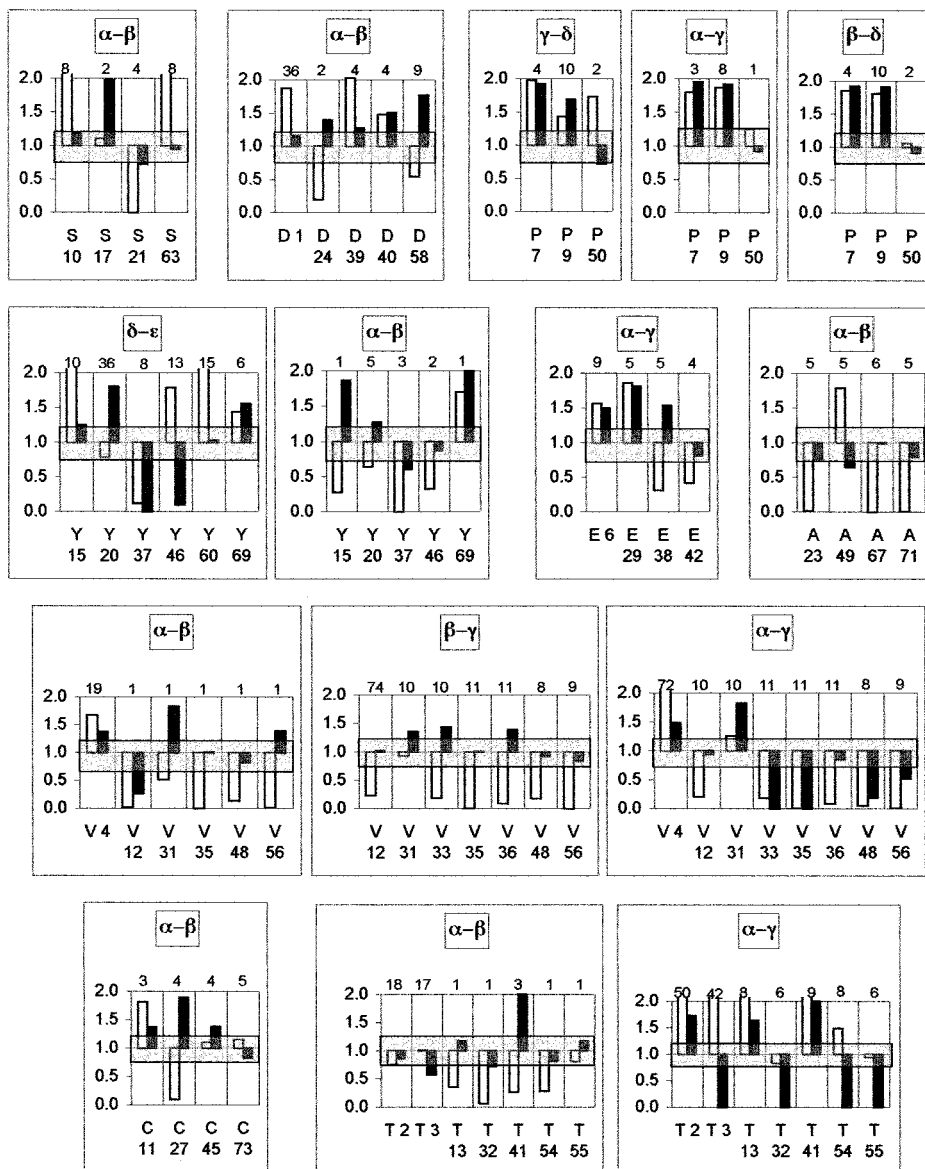


Figure 3. The autoscaled paramagnetic attenuations, A_i , calculated for all the well-resolved correlations of selected tendamistat-type residues (dark bars), compared with the exposed surface area, ESA_i , of the corresponding atoms. The ESA_i calculations have been performed on the solution structure of the protein (PDB code 4AIT), as discussed in the text. The shadowed areas of the histograms represent the standard deviation calculated on all the A_i data. The sum of the rmsd of the atomic positions in the nine structures contained in the 4AIT Protein Data Bank file, see the text and Kline et al. (1988), is reported for each group of atoms and shown on top of each histogram bar. Broken bars indicate out of scale ESA_i values.

of V12, N25, Y37 and G59; (ii) the δ and ϵ hydrogen connectivity of Y37 and Y46; and (iii) the α and γ hydrogen connectivity of V33, V35, V48, T3, T32, T54 and T55. The agreement with the corresponding ESA_i values is very good, except for Y46 and all thronyl residues. The very high rmsd value of the atomic positions observed for the α and γ hydrogens of T3

might account for the corresponding A_i versus ESA_i discrepancy. A high local mobility, in fact, is expected to weaken the paramagnetic perturbation.

The fact that Y46, T54 and T55 are located in the same area of the tendamistat surface suggests a reduced accessibility of the probe to this molecular moiety, due to the presence of water molecules

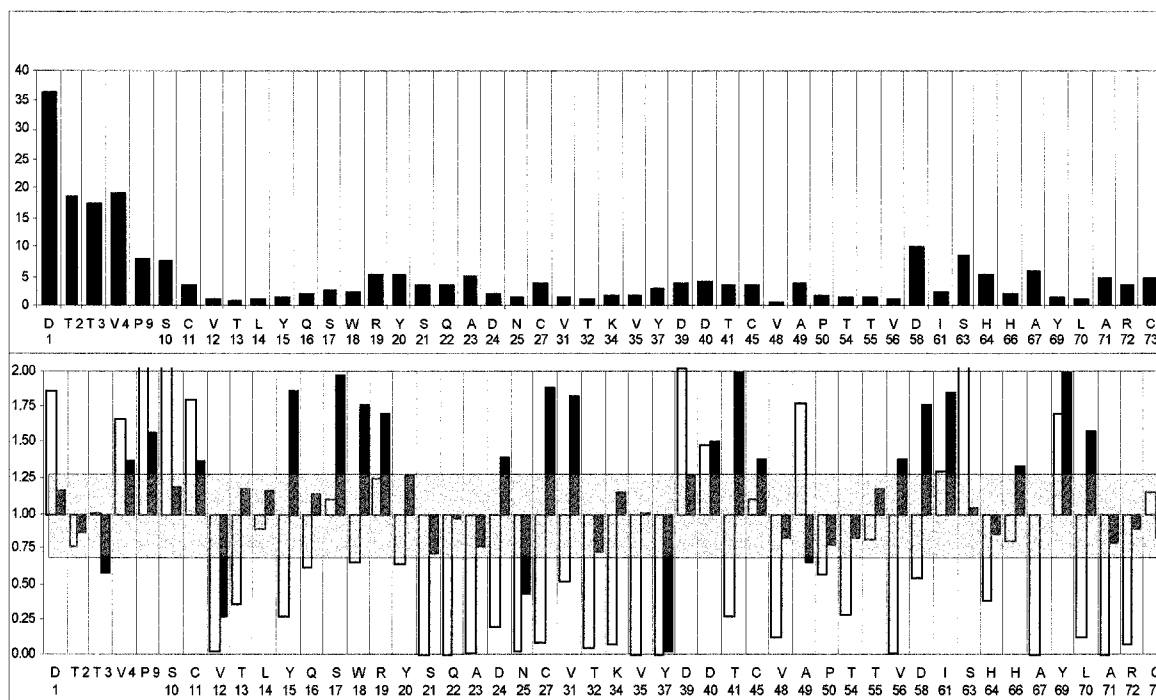


Figure 4. As in Figure 3, but the comparison of A_i with ESA_i is done for all the well-resolved α - β correlations found in the tendamistat TOCSY spectra of Figure 2. The α - α correlation is given for G59. The sum of the rmsd of the atomic position of α and β hydrogens is shown in the upper histogram.

tightly bound to the solvent-exposed hydroxyl groups of these residues. Similarly, bound water molecules could explain also the T32 α - γ discrepancy.

On the other hand, the most attenuated correlations are observed for the hydrogens, which belong to the residues forming the contiguous surface regions shown in Figure 5. The paramagnetic effects induced by TEMPOL define surface patches of close approach of the probe. In many cases this finding can be simply explained by steric considerations, since, in general, a high ESA_i corresponds to a high A_i . However, a more interesting insight comes from the discrepancies entailing high A_i versus low ESA_i . Outstanding discrepancies are in fact observed for (i) the α and β hydrogen connectivity of Y15, S17, W18, C27, V31, T41, V56, D58 and L70, (ii) the α and γ hydrogen connectivity of V31 and E38, (iii) the β and γ hydrogen connectivity of V31, V33 and V36 and (iv) the δ and ϵ hydrogen connectivity of Y20.

It is of primary interest to notice from these data that the largest patch of close approach of TEMPOL is centred around the 18–20 tendamistat fragment which is considered responsible for the α amylase inhibition (Marchiusi et al., 1996). Significantly, the same active

site region of tendamistat exhibits the most striking differences upon comparison between the crystal and the NMR-restrained solution structure (Billeter et al., 1989).

Only in the case of the V33 β - γ correlation can the explanation of the experimental data resort to the high rmsd, which suggests the possibility of local conformations with an accessibility higher than that of structure I used for the ESA_i calculations. All the other anomalous high TEMPOL effects, except for the isolated V56 and C45 residues, are related to hydrogens, which are partially exposed and connected to form two small surface patches.

The deviations of the experimental A_i of the side chain resonances with respect to the calculated ESA_i suggests the possibility that their TEMPOL-induced paramagnetic attenuation reflects also factors other than the static conformational exposure. Such a hypothesis is supported by the observation that, out of the 63 TEMPOL-induced effects which fall outside the statistical limits of average behaviour, 30 A_i 's are consistent with the corresponding ESA_i 's, while 10 A_i are much lower than ESA_i and 23 A_i are much higher than the corresponding ESA_i counterparts.

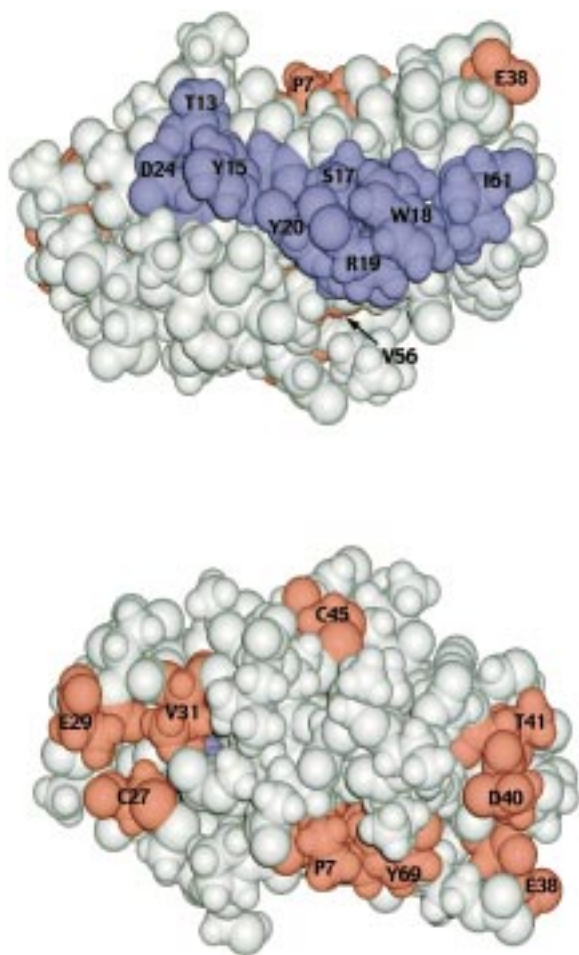


Figure 5. Two complementary views of the tendamistat solution structure: all the residues which exhibit paramagnetic attenuations above the standard deviation limit are coloured. In purple are shown all the residues located in the large surface patch, including the protein active site.

The presence of tightly bound water molecules could prevent a close approach of the paramagnetic probe to the protein surface, as in the case of the amino and carboxy terminal residues T2, T3 and C73 or for Y46, P50, T54 and T55. On the contrary, a favourable competition with the solvent could account for the opposite behaviour of all the residues shown in Figure 5. This favourable competition may be correlated with a decreased extent of hydrophobic ordering of the protein solvation shell. It should be noted also that, with a few exceptions, no correlation exists between anomalous paramagnetic effects and large rmsd values of the hydrogen coordinates.

Thus, whenever the protein solution structure is known, a discussion of the anomalously high or low

paramagnetic attenuations compared to the computed static accessibility may yield information on the dynamic accessibility of the protein surface and on the stability of its solvation sphere. This conclusion should hold true both for side chain and backbone resonances. Furthermore, the fact that the active site of tendamistat is particularly accessible by the spin-probe is consistent with our previous observations on the NH-H α correlations of lysozyme W63 (Esposito et al., 1992) and BPTI N15 (Molinari et al., 1997). It is interesting to note that also in these cases the most affected hydrogens are located at the active site. Since the characteristics of the active sites of tendamistat, lysozyme and BPTI are very different and the spin-probe is a chemical species which greatly differs from any of the specific ligands of the three proteins, it can be suggested that the solvent dynamics are essential in favouring non-specific molecular approaches to the protein active sites. TEMPOL-induced paramagnetic attenuations of proton resonances in multidimensional NMR spectra may be consistently explained only by assuming that protein active sites are regions of the molecular surface where accessibility is in general higher than in the other surface regions. These findings are in total agreement with the diffusion of small organic molecules observed in protein single crystals (Ringe, 1995; Mattos et al., 1996) and in solution (Liepinsh et al., 1997).

The high accessibility of protein active sites could be viewed as the consequence of a reduced presence of structured water and of the simultaneous preferential diffusion of non-water molecules. The high sampling frequency ensuing thereof should enhance the occurrence probability of productive intermolecular presentation, necessary for functional recognition processes. Overall, the approach of non-aqueous ligand to the protein surface should feature a very inhomogeneous pattern, with preferential flow vortexes directed towards the active site.

Since, in addition to the overall solvent exposure based on statistic collisions, TEMPOL appears also capable of probing an uneven accessibility distribution on a protein surface based on solvation dynamics, as a final remark, it can be suggested that the spin-probe can highlight those residues which are critical for the recognition process and, hence, for the design of protein mutants of modulated biological activity.

Acknowledgements

N.N. thanks the Italian C.N.R. (Progetto Strategico Biologia Strutturale) and MURST (ex40% Progetto Biologia Strutturale) for the financial support, the University of Siena for the 60% contribution and Francesco Niccolai to be born after the completion of this manuscript.

References

- Balacco, G. (1994) *J. Chem. Inf. Comput. Sci.*, **34**, 1235–1241.
- Billeter, M., Kline, A.D., Braun, W., Huber, R. and Wüthrich, K. (1989) *J. Mol. Biol.*, **206**, 677–689.
- Campbell, I.D. and Dwek, R.A. (1984) *Biological Spectroscopy*, Benjamin Cummings, Menlo Park, CA, pp. 190–194.
- Clare, G.M., Bax, A., Wingfield, P.T. and Gronenborn, A. (1990) *Biochemistry*, **29**, 567–574.
- Dalvit, C., Ramage, P. and Hommel, U. (1998) *J. Magn. Reson.*, **131**, 148–153.
- Dalvit, C. (1999) 2nd International Workshop on Structural Characterization of Proteins by NMR, X-Ray Diffraction and Computational Methods, Verona, Italy.
- Esposito, G., Molinari, H., Motta, A. and Niccolai, N. (1989) Proc. XXIII Convegno Nazionale GDRM, Cagliari, Italy, p. 11.
- Esposito, G., Lesk, A.M., Molinari, H., Motta, A., Niccolai, N. and Pastore, A. (1992) *J. Mol. Biol.*, **224**, 659–670.
- Esposito, G., Molinari, H., Niccolai, N., Pegna, M. and Zetta, L. (1993) *J. Chem. Soc., Perkin Trans. II*, 1531–1534.
- Girvin, M.E. and Fillingame, R.H. (1995) *Biochemistry*, **34**, 1635–1645.
- Kline, A.D. and Wüthrich, K. (1985) *J. Mol. Biol.*, **183**, 503–507.
- Kline, A.D. and Wüthrich, K. (1986) *J. Mol. Biol.*, **192**, 869–890.
- Kline, A.D., Braun, W. and Wüthrich, K. (1988) *J. Mol. Biol.*, **204**, 675–724.
- Liepinsh, E. and Otting, G. (1997) *Nat. Biotechnol.*, **15**, 264–268.
- Marchiusi, M., Vertesy, L., Huber, R. and Wiegand, G. (1996) *J. Mol. Biol.*, **260**, 409–421.
- Mattos, C. and Ringe, D. (1996) *Nat. Biotechnol.*, **14**, 595–599.
- Molinari, H., Esposito, G., Pegna, M., Ragona, L., Niccolai, N. and Zetta, L. (1997) *Biophys. J.*, **73**, 382–396.
- Morris, G.A. and Freeman, R. (1978) *J. Magn. Reson.*, **29**, 433–462.
- Niccolai, N., Esposito, G., Mascagni, P., Motta, A., Bonci, A., Rustici, M., Scarselli, M., Neri, P. and Molinari, H. (1991) *J. Chem. Soc., Perkin Trans. II*, 1453–1457.
- Niccolai, N., Valensin, G., Rossi, C. and Gibbons, W.A. (1982) *J. Am. Chem. Soc.*, **104**, 1534–1537.
- Otting, G. and Wüthrich, K. (1989) *J. Am. Chem. Soc.*, **111**, 1871–1875.
- Otting, G., Liepinsh, E. and Wüthrich, K. (1991) *Science*, **254**, 974–980.
- Petros, A.M., Mueller, L. and Kopple, K.D. (1990) *Biochemistry*, **29**, 10041–10048.
- Pflugrath, J., Wiegand, E., Huber, R. and Vertesy, L. (1986) *J. Mol. Biol.*, **189**, 383–386.
- Rance, M. (1987) *J. Magn. Reson.*, **74**, 557–564.
- Ringe, D. (1995) *Curr. Opin. Struct. Biol.*, **5**, 825–829.
- Wüthrich, K. (1998) *Nat. Struct. Biol., NMR supplement*, 492–495.